

Generation of two identical photons from a quantum dot in a microcavity

E. del Valle,¹ A. Gonzalez-Tudela,² E. Cancellieri,² F. P. Laussy,³ and C. Tejedor²

¹*Physikdepartment, TU München, James-Frank-Str. 1, 85748 Garching, Germany*

²*Física Teórica de la Materia Condensada, Universidad Autónoma de Madrid, 28049, Madrid, Spain*

³*Walter Schottky Institut, Technische Universität München, Am Coulombwall 3, 85748 Garching, Germany*

(Dated: December 1, 2021)

We propose and characterize a two-photon emitter in a highly polarised, monochromatic and directional beam, realized by means of a quantum dot embedded in a linearly polarized cavity. In our scheme, the cavity frequency is tuned to half the frequency of the biexciton (two excitons with opposite spins) and largely detuned from the excitons thanks to the large biexciton binding energy. We show how the emission can be Purcell enhanced by several orders of magnitude into the two-photon channel for available experimental systems.

Sources of pairs of identical photons are fundamental devices in quantum metrology [1], quantum communication and cryptography [2–4], linear-optics quantum computation [5, 6], and even for fundamental tests of quantum mechanics like hidden variables interpretations [7, 8]. A number of devices have been proposed and experimentally demonstrated with atomic gases [9] or nonlinear crystals [1]. The realization of such devices, however, is a highly nontrivial task since, in order to be useful, the generated photons need to be almost identical, extremely narrow-band and be generated with an extremely high repetition rate. Some of us and coworkers have recently proposed a scheme based on a single quantum dot embedded in a microcavity [10], which theoretically fulfils all the above requirements and, moreover, is particularly promising for scalable technological implementations. The principle relies on the biexciton (the occupation of the quantum dot by two excitons of opposite spins) being brought in resonance with twice the cavity photon energy. Thanks to the large biexciton binding energy, single-photon processes are detuned and are thus effectively suppressed, while simultaneous two-photon emission is Purcell enhanced. This effect has been recently demonstrated experimentally [11]. In the experiment, as in the initial proposal [10], the signature for the two-photon emission is a strong emission enhancement of the cavity mode when hitting the biexciton two-photon resonance. Because of incoherent excitation used in both the theoretical proposal and its experimental realization, the quantum character of the two-photon emission is not directly demonstrated nor quantified [12]. Here, we upgrade to a configuration that is nowadays experimentally accessible, where the quantum dot is initially prepared in a pure biexciton state [13–15], and analyze in details the underlying microscopic mechanisms, demonstrating the perfect two-photon character of the emission beyond a mere enhancement at the expected energy. We show how the two-photon state is created by the system in a chain of virtual processes that cannot be broken apart in physical one-photon states. Our understanding is analytical and allows for optimisation of a practical setup, enabling the realization of a practical source of two simultaneous

and indistinguishable photons in a monolithic semiconductor device.

The characteristic spectral profile of the cavity-assisted two-photon emission is shown in Fig. 1, with a central peak that is strongly enhanced at the two-photon resonance, corroborating its two-photon character, and surrounded by standard (single-photon) de-excitation [10, 11]. The photon-pair peak is spectrally narrow and isolated from the other events, that can never be completely avoided, so the source is appealing on practical grounds. The Hamiltonian of the system reads [10]:

$$H(t) = (\omega_a - \omega_L) a^\dagger a + \sum_{i=\uparrow, \downarrow} (\omega_X - \omega_L) \sigma_i^\dagger \sigma_i - \chi \sigma_\uparrow^\dagger \sigma_\uparrow \sigma_\downarrow^\dagger \sigma_\downarrow + \sum_{i=\uparrow, \downarrow} \left[g_i (a^\dagger \sigma_i + a \sigma_i^\dagger) + \Omega_i(t) (\sigma_i + \sigma_i^\dagger) \right], \quad (1)$$

where we have included $i = \uparrow, \downarrow$ the spin-up and spin-down degrees of freedom for the excitonic states σ_i (fermions) with common frequency ω_X and a the cavity field annihilation operator (boson) with frequency ω_a . The cavity mode can have a strong polarization, say linearly polarized in the horizontal direction for a photonic crystal, a case we shall assume in the following. The biexciton binding energy χ allows to bring the biexciton energy ω_B in resonance with the two-photon energy while detuning all other excitonic emissions from the cavity mode. It is red (blue) shifted if the biexciton is “bound” (“antibound”), giving rise to a positive $\chi > 0$ (negative $\chi < 0$) binding energy $\chi = 2\omega_X - \omega_B$. Our scheme works with both the bound and antibound biexciton. Without loss of generality, we assume $\chi > 0$, with the added advantage of being less affected by pure dephasing and coupling to phonons, that we neglect [16]. This binding energy is typically large ($\chi \approx 400 \mu\text{eV}$) as compared to splittings between excitonic states ($\approx 10 \mu\text{eV}$) [11], which is ideal for our purpose. We will assume an equal coupling of both excitons to the linearly polarized mode of the cavity, $g_\uparrow = g_\downarrow = g/\sqrt{2}$, and take g as the unit in the remaining of the text. The Hilbert space of the quantum dot is spanned, in its natural basis of circularly polarised states, by the ground $|G\rangle$, spin-up $|\uparrow\rangle$, spin-down

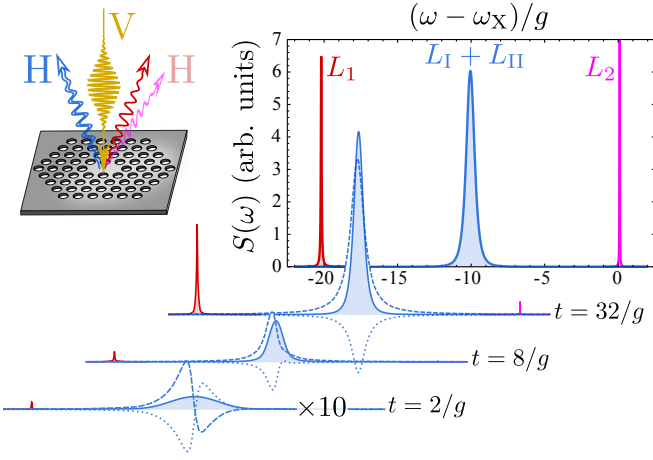


FIG. 1. (color online) Cavity spectra of emission $S(t, \omega)$ at the two-photon resonance for different times (unframed) and integrated over all times (framed). They feature the 2P peak at $\omega_a \approx -\chi/2$ (central, blue) and the two 1P peaks at $\omega_1 \approx -\chi$ (left, red) and $\omega_2 \approx 0$ (right, pink). The 2P peak cannot be decomposed into two physical processes. Parameters: $\chi = 20g$, $\kappa = g$, $\gamma = 5 \times 10^{-4}g$.

$|\downarrow\rangle$ and biexciton $|B\rangle$ states. In the linearly polarised basis, the excitonic states are $|H\rangle = (|\uparrow\rangle + |\downarrow\rangle)/\sqrt{2}$ and $|V\rangle = (|\uparrow\rangle - |\downarrow\rangle)/\sqrt{2}$. The dot-cavity joint Hilbert space includes the photonic number n : $|j, n\rangle$, where $j = G, V, H$ and B , with $n \in \mathbb{N}$.

The quantum dot is excited by a laser of amplitude $\Omega_i(t)$ and frequency ω_L , that brings it in the biexciton state through two-photon absorption. This can be realised via an appropriate pulse or sequence of pulses. The laser polarization should be taken orthogonal to that of the cavity, $\Omega_\uparrow(t) = -\Omega_\downarrow(t) = \Omega(t)/\sqrt{2}$, so that the latter is not affected by the excitation process. Coherent control of the biexciton has been reported in several works [13–15] and we will assume the biexciton in an empty cavity, $|B, 0\rangle$, as the initial state following the pulse. The laser frequency should be set to match the two-photon resonance, $\omega_L = \omega_B/2 = \omega_X - \chi/2$. With the previous considerations, the Hamiltonian in the basis of linearly polarized states reads:

$$H = \omega_a a^\dagger a + \omega_X (|H\rangle \langle H| + |V\rangle \langle V|) + (2\omega_X - \chi) |B\rangle \langle B| + g \left[a^\dagger (|G\rangle \langle H| + |H\rangle \langle B|) + \text{h.c.} \right], \quad (2)$$

where it now appears explicitly that the cavity couples only to its corresponding linear polarization (H). Dissipation affects the bare states, i.e., in the spin-up/spin-down basis, yielding a master equation:

$$\partial_t \rho = i[\rho, H] + \frac{\kappa}{2} \mathcal{L}_a(\rho) + \frac{\gamma}{2} \sum_{i=\uparrow, \downarrow} \left[\mathcal{L}_{|G\rangle \langle i|} + \mathcal{L}_{|i\rangle \langle B|} \right](\rho), \quad (3)$$

where $\mathcal{L}_c(\rho) = 2c\rho c^\dagger - c^\dagger c\rho - \rho c^\dagger c$, with κ the cavity losses and γ the exciton relaxation rates. Fig. 2 shows

the configuration of levels involved in the biexciton de-excitation, that is truncated self-consistently. The coherent coupling (g) is represented by bidirectional (green) arrows, spontaneous decay (γ) by straight (gray) arrows and cavity decay (κ) by curly (blue) arrows, each of them linking in a reversible (g) or irreversible (γ, κ) way the different levels.

A *one-photon resonance* (1PR) is realized when the cavity is set at resonance with one of the excitonic transitions: $|B, 0\rangle \rightarrow |H, 0\rangle$ with frequency $\omega_1 \approx \omega_B - \omega_X$ or $|H, 0\rangle \rightarrow |G, 0\rangle$ with frequency $\omega_2 \approx \omega_X$. The resonant single-photon emission is then enhanced into the cavity mode according to the conventional scenario [17], with a Purcell decay rate $\gamma_P = 4g^2/\kappa$. A *two-photon resonance* (2PR) is realized when the transition $|B, 0\rangle \rightarrow |G, 0\rangle$ matches energetically the emission of two cavity photons [10]:

$$\omega_a \approx \omega_X - \chi/2 \quad \text{with} \quad \chi \gg g, \kappa, \gamma. \quad (4)$$

This process also benefits from Purcell enhancement. In fact, if the decay rates γ and κ are small enough, two-photon Rabi oscillations between states $|B, 0\rangle$ and $|G, 2\rangle$ are even realized, with a characteristic frequency $g_{2P} \approx 4g^2/(\sqrt{2}\chi)$ [10]. Note that in Eq. (4), we have neglected the small Stark shifts $\sim g_{2P}$, which should be taken into account to achieve maximum Rabi amplitude. In this text, to remain within experimentally achievable configurations, we consider systems in strong coupling, $g \gtrsim \kappa$, but not so much that the two-photon oscillations actually take place, that is, we remain within the 2P weakly coupled regime, $4g_{2P} \ll \kappa$. The one-photon Rabi oscillations (e.g., $|B, 0\rangle \leftrightarrow |H, 1\rangle$) still take place at the frequency g but, as they are largely detuned, the coupling strength effectively reduces to $g_{1P} \approx g/\sqrt{1 + [\chi/(\gamma + \kappa)]^2} \approx g\kappa/\chi$ [18].

To characterize and analyze the main output of the system, shown in Fig. 1, we study the time-resolved power spectrum $S(t, \omega) \propto \Re \int_0^t dT \int_0^{t-T} d\tau e^{i\omega\tau} \langle a^\dagger(T) a(T + \tau) \rangle$ [19] that we compute as:

$$S(t, \omega) = \frac{1}{\pi} \sum_{\alpha \in \{1, 2, I, II, \dots\}} \frac{L_\alpha(\gamma_\alpha/2) - K_\alpha(\omega - \omega_\alpha)}{(\gamma_\alpha/2)^2 + (\omega - \omega_\alpha)^2}, \quad (5)$$

where we emphasised in the sum four dominant processes labelled 1, 2, I and II (results below include all processes). Each α corresponds to a transition in the system, characterised by its frequency (ω_α) and broadening (γ_α) on the one hand, which allow us to identify its microscopic origin, as discussed below, and its intensity L_α and interferences with other transitions K_α [18] on the other hand. The time dependent spectra of emission can be measured experimentally with a streak camera [20].

There are two channels of de-excitation: via the cavity mode (through the annihilation of a photon a) or via spontaneous emission into the leaky modes (related to the

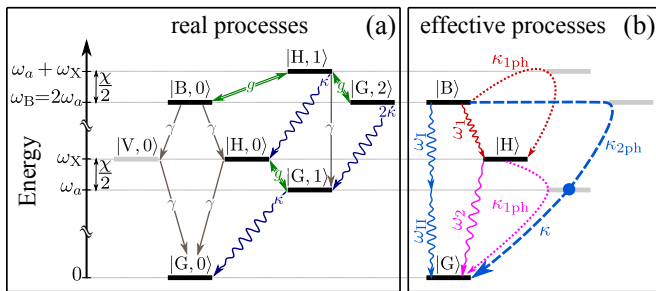


FIG. 2. (color online) Level scheme of a quantum dot coupled to a cavity mode with linear polarization H at the 2PR. In (a), the microscopic configuration and in (b) the effective processes taking place in the de-excitation of the biexciton. Those involving the cavity are, on the one hand, through the emission of two real and distinguishable photons ω_1 and ω_2 (in dotted red and pink), and, on the other hand, through the simultaneous emission of one two-photon state at ω_a (in dashed blue), labelled $\omega_{I,II}$.

four excitonic lowering operators). With the biexciton state in an empty cavity, $|B, 0\rangle$, as the initial condition, we identify three de-excitation mechanisms of the system. We now describe them in turns.

i) The first decay route is a cascade of two spontaneous emissions, from $|B\rangle$ to $|H\rangle$ (or $|V\rangle$) in a first time, and then from $|H\rangle$ (or $|V\rangle$) to $|G\rangle$ in a second time, as shown in straight (gray) lines in Fig. 2(a). This decay into leaky modes is at the excitonic energies, ω_1 , ω_2 , and is a direct process with a straightforward microscopic origin as a transition between two states. Each process happens at the rate γ , so that, as far as the biexciton is concerned, its total rate of de-excitation through this channel is 2γ . The effect of this channel is to reduce the efficiency of de-excitation through the cavity mode, which is the one of interest. This can be kept small by choosing a system with a small γ .

ii) The second decay route is another cascade of one-photon emissions, but now through the cavity mode, namely from $|B\rangle$ to $|G\rangle$ passing by $|H\rangle$. It is shown in dotted lines in Fig. 2(b). It effectively amounts to two consecutive photons into the cavity mode at the excitonic energies ω_1 and ω_2 , also shown (with the same color code) in Fig. 2(b), but the microscopic origin is now more complex, as it involves virtual intermediate states. The first photon (1) is emitted through the process $|B, 0\rangle \xrightarrow{|H,1\rangle} |H, 0\rangle$, via the off-resonant (“virtual”) state $|H, 1\rangle$ and the second (2), similarly through the process $|H, 0\rangle \xrightarrow{|G,1\rangle} |G, 0\rangle$. These transitions occur at the Purcell rate $\kappa_{1P} \approx 4g_{1P}^2/\kappa \approx T_{1P}^2\kappa$, where $T_{1P} = 2g/\chi$ is the effective mixing parameter between states $|B, 0\rangle$ – $|H, 1\rangle$ and $|H, 0\rangle$ – $|G, 1\rangle$. The positions and broadenings are more precisely given by $\omega_1 \approx -\chi - 2g^2/\chi$, $\omega_2 \approx 2g^2/\chi$ and $\gamma_1 \approx 3\gamma$, $\gamma_2 \approx \gamma$.

iii) Finally, the central event in our proposal is formed

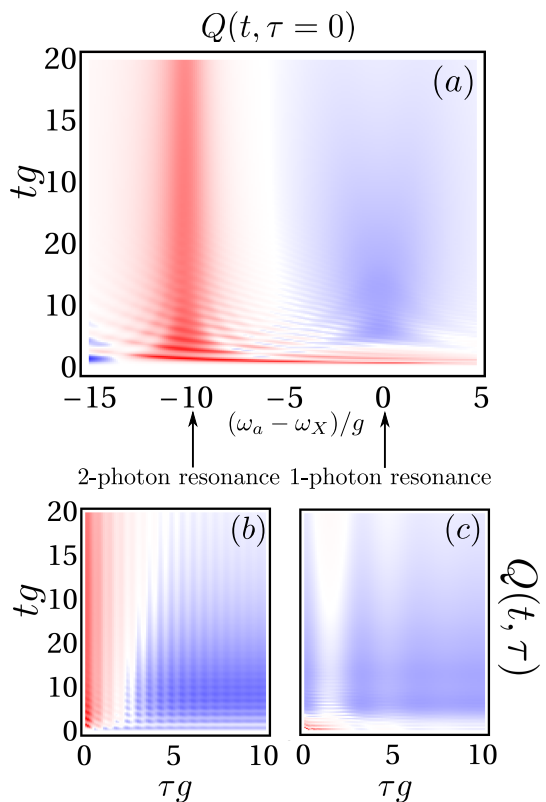


FIG. 3. (color online) (a) Mandel parameter $Q(t, \tau = 0)$ as a function of the cavity frequency ω_a , for a set of typical parameters ($\chi = 20g$, $\kappa = 0.5g$ and $\gamma = 5 \times 10^{-3}g$). $Q(t, \tau)$ is shown below at the two relevant resonances, two-photon (a) and one-photon (b). There is a change in the statistics from antibunching < 0 (1PR), colored in blue, to bunching > 0 (2PR), colored in red.

by the third channel of de-excitation of the biexciton, namely, the emission into the cavity mode of two simultaneous and indistinguishable photons with a frequency very close to that of the cavity $\omega_I \approx \omega_{II} \approx \omega_a$. This process is sketched by the single dashed (blue) line in Fig. 2(b), with an intermediate step marked by a point at $|G, 1\rangle$. Effectively, this amounts to the generation of a two-photon state, represented by the two curly transitions $\omega_{I,II}$ in Fig. 2(b). The two indices I and II strictly correspond to transitions that arise in the spectral decomposition (5), namely, $|B, 0\rangle \xrightarrow{|G,2\rangle} |G, 1\rangle$ for the first sequence of events, I, and the closing of the path, $|G, 1\rangle \rightarrow |G, 0\rangle$, for the second transition, II. Although we have used I and II in Fig. 2 to label the two photons for the sake of illustration, these two photons are indistinguishable and cannot be interpreted as real events taken in isolation in association with the above sequences of transitions. Indeed, each event gives rise to an unphysical spectrum (assuming negative values) and only when both processes are taken together, they interfere to sum to a physical spectrum which can be interpreted as a

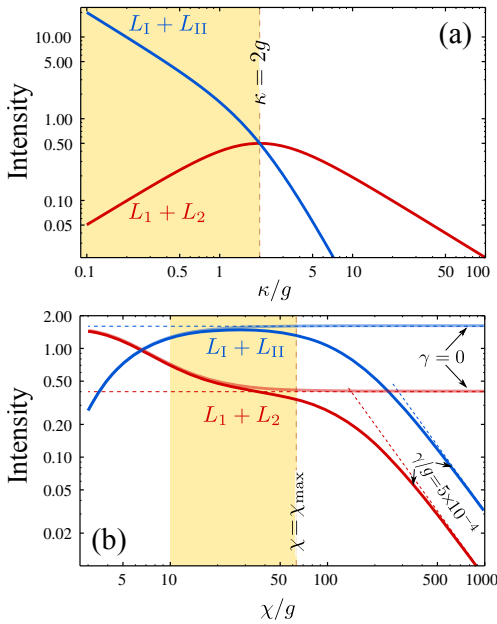


FIG. 4. (color online) (a) Intensity $L_I + L_{II}$ of emission in the 2P channel (blue) and $L_1 + L_2$ in the two 1P channels (red) as a function of κ in the ideal case of nonradiative emission, $\gamma = 0$ and $\chi \rightarrow \infty$. The shaded (yellow) area $\kappa < 2g$ shows the region where the 2P emission dominates. (b) Same as above for $\kappa = g$ as a function of χ , that must be large enough so that 1P are suppressed and small enough to maintain a high cavity emission efficiency in the realistic case of nonzero γ .

probability of (two-photon) detection. This decomposition of the two-photon (central) peak is shown in Fig. 1 in the time-dependent spectra, with the process I shown in a dotted line and II in dashed line. They sum to the physical (observable) peak, in solid line. Both peaks grow together in time and develop an asymmetry, one (I) being completely positive, the other (II) completely negative. None, not even the fully positive peak, can be observed in isolation. In contrast, the single-photon peaks on both sides (red and pink), are formed by single, isolated transitions, showing their real (as opposed to virtual) nature. The two-photon emission is enhanced by the Purcell rate $\kappa_{2P} \approx 4g_{2P}^2/(2\kappa) \approx T_{2P}^2 2\kappa$, where $T_{2P} = g_{2P}/\kappa$ is the effective mixing parameter between states $|B, 0\rangle$ - $|G, 2\rangle$. We use 2κ because this is the decay rate of the intermediate state $|G, 2\rangle$. One transition appears, more precisely, at $\omega_I \approx -\chi/2 + 2g^2/\chi$ with broadening $\gamma_I \approx \kappa + 2\gamma$ (this is the sum of the decay that initial and final states suffer, $|B, 0\rangle$ and $|G, 1\rangle$). The other transition (II) stems from the direct process $|G, 1\rangle \rightarrow |G, 0\rangle$. This transition appears at $\omega_{II} \approx -\chi/2 - 2g^2/\chi$ with broadening $\gamma_{II} \approx \kappa$.

Another proof of the two-photon character is given by the time-dependent spectrum, Fig. 1. Whereas the single-photon events grow in succession—first the L_1 peak, that populates the state $|H\rangle$, which subsequently decays to $|G\rangle$, forming the L_2 peak—the two photon peak

arises from the joint and simultaneous contribution of the I and II processes. In fact, one can show that at the 2PR, $L_I + L_{II} \approx 2\langle a^\dagger{}^2 a^2 \rangle$, linking directly the intensity of the peak with the two-photon emission probability. This can be brought to the experimental test by resolving the photon statistics in time, $g^{(2)}(t, \tau) = \langle a^\dagger(t)a^\dagger(t+\tau)a(t+\tau)a(t) \rangle / [n_a(t)n_a(t+\tau)]$. We use the Mandel Q -parameter, $Q(t, \tau) = n_a(t)(g^{(2)}(t, \tau) - 1)$, that changes sign (negative for anticorrelations). This is shown in Fig. 3. The main panel, (a), shows a strong and sharp bunching of the emission when the cavity hits the two-photon resonance (meaning that photons come together, and in our case, in pairs), while it is antibunched in other cases (photons coming separately). What is remarkable of the two photon emission is that it is consistently bunched at all times: while the system can emit at any time, when it does, it emits the two photons together. In contrast, the 1PR emission which is antibunched as expected when the process is isolated, also has the possibility to be bunched by fortuitous joint emission of two photons. This is the case when $\omega_a = \omega_2$, the cavity is then in resonance with the lower transition, that can start only as a successor of the upper transition resulting in high probability for two photons detection, but only at very early times, since one photon is a precursor of the other one in a cascade of two otherwise distinguishable events. The proof is complete with the autocorrelation time τ , shown in panels (b) and (c), further demonstrating that in the 2PR emission, the two photons arrive at zero time delay (the emission being less likely again at nonzero delay).

Now that we have demonstrated from various points of view the two-photon character of the central peak, we aim to maximise it as compared to all other de-excitation channels. There are three key parameters to enhance the 2P emission, κ , γ and χ . The case $\gamma = 0$ and $\chi \rightarrow \infty$ is the ideal configuration, where all the emission goes through the cavity:

$$I_a = \int_0^\infty \langle a^\dagger a \rangle(t) dt = 2/\kappa, \quad (6)$$

which is redistributed between the two possible decay paths as:

$$L_1 + L_2 \approx \frac{\kappa_{1P}}{\kappa_{1P} + \kappa_{2P}} I_a \approx \frac{2}{\gamma_P + \kappa}, \quad (7a)$$

$$L_I + L_{II} \approx \frac{\kappa_{2P}}{\kappa_{1P} + \kappa_{2P}} I_a \approx \frac{2\gamma_P/\kappa}{\gamma_P + \kappa}. \quad (7b)$$

This is shown in Fig. 4(a), where we see that the 2P emission dominates over the 1P when $\kappa < 2g$ (shaded in yellow in Fig. 4(a)), since in this case $\kappa_{2P} > \kappa_{1P}$. For cavities with high enough quality factor (small κ), the 2P emission is over four orders of magnitude higher than the 1P, showing that the device is extremely efficient with favourable technological parameters.

When γ is nonzero, the situation of experimental interest, but still is the smallest parameter ($\ll \kappa, g \ll \chi$), the channel of decay it opens leads to:

$$I_a = \int_0^\infty n_a(t) dt = \frac{\gamma_P(\gamma_P + \kappa)}{\gamma\chi^2}, \quad (8)$$

which is now redistributed between the two cavity decay paths as an increasing function of χ^{-2} :

$$L_I + L_2 \approx \frac{\kappa_{1P}}{\kappa_{1P} + \kappa_{2P} + 2\gamma} I_a \approx \frac{\gamma_P \kappa}{\gamma\chi^2}, \quad (9a)$$

$$L_I + L_{II} \approx \frac{\kappa_{2P}}{\kappa_{1P} + \kappa_{2P} + 2\gamma} I_a \approx \frac{\gamma_P^2}{\gamma\chi^2}. \quad (9b)$$

This nonzero γ case is shown in Fig. 4(b), where the ideal situation can be recovered in a region of χ bounded by above by:

$$\chi_{\max} = \min(2g\sqrt{\kappa/(2\gamma)}, 4g^2/\sqrt{2\kappa\gamma}), \quad (10)$$

that follows from $2\gamma = \min(\kappa_{1P}, \kappa_{2P})$. Above χ_{\max} , the 2P emission still dominates over 1P emission but efficiency is spoiled, according to Eqs. (9), that are shown in dashed tilted lines.

In conclusion, we have presented a scheme where the biexciton is in two-photon resonance with a microcavity mode, as an efficient two-photon source, both in terms of the purity of the two-photon state and of its emission efficiency. The timescale for two-photon emission, that limits the repetition rate, is of the order of κ_{2P}^{-1} . The quantum character of the two-photon emission is demonstrated theoretically by a detailed analysis of all the processes involved in the biexciton de-excitation, which also allows us to find analytically the optimum conditions for its realization. We have shown that the two-photons are emitted simultaneously with no delay in the autocorrelation time. Experimentally, the ultimate proof of indistinguishability can be obtained by directing the central peak to a beam-splitter, which half of the time will separate the photon pair into two ports that can then be fed in an Hong-Ou-Mandel interferometer.

We thank F. Troiani, D. Sanvitto, A. Laucht and J. J. Finley for discussions. We acknowledge support from the Emmy Noether project HA 5593/1-1 (DFG), the Marie Curie IEF ‘SQOD’, the Spanish MICINN (MAT2008-01555 and CSD2006-00019-QOIT) and CAM (S-2009/ESP-1503). A.G.-T. thanks the FPU program (AP2008-00101) from the Spanish Ministry of Education.

-
- [1] T. Nagata, R. Okamoto, J. L. O’Brien, K. Sasaki, and S. Takeuchi, *Science* **316**, 726 (2007)
 - [2] C. Simon, H. de Riedmatten, M. Afzelius, N. Sangouard, H. Zbinden, and N. Gisin, *Phys. Rev. Lett.* **98**, 190503 (2007)
 - [3] J. I. Cirac, P. Zoller, H. J. Kimble, and H. Mabuchi, *Phys. Rev. Lett.* **78**, 3221 (1997)
 - [4] L.-M. Duan, M. D. Lukin, J. I. Cirac, and P. Zoller, *Nature* **414**, 413 (2001)
 - [5] P. Kok, W. J. Munro, K. Nemoto, T. C. Ralph, J. P. Dowling, and G. J. Milburn, *Rev. Mod. Phys.* **79**, 135 (2007)
 - [6] B. P. Lanyon, T. J. Weinhold, N. K. Langford, J. L. O’Brien, K. J. Resch, A. Gilchrist, and A. G. White, *Phys. Rev. Lett.* **100**, 060504 (2008)
 - [7] A. Aspect, P. Grangier, and G. Roger, *Phys. Rev. Lett.* **49**, 91 (1982)
 - [8] D. Collins, N. Gisin, N. Linden, S. Massar, and S. Popescu, *Phys. Rev. Lett.* **88**, 040404 (2002)
 - [9] J. K. Thompson, J. Simon, H. Loh, and V. Vuletic, *Science* **313**, 74 (2006)
 - [10] E. del Valle, S. Zippilli, F. P. Laussy, A. Gonzalez-Tudela, G. Morigi, and C. Tejedor, *Phys. Rev. B* **81**, 035302 (2010)
 - [11] Y. Ota, S. Iwamoto, N. Kumagai, and Y. Arakawa, arXiv:1107.0372 (2011)
 - [12] The Authors of Ref. [11] also realize this limitation and speculate on the scheme that we analyze here in details. Stop
 - [13] A. Dousse, J. Suffczynski, A. Beveratos, O. Krebs, A. Lemaitre, I. Sagnes, J. Bloch, P. Voisin, and P. Senellart, *Nature* **466**, 217 (2010)
 - [14] S. Stuffer, P. Machnikowski, P. Ester, M. Bichler, V. M. Axt, T. Kuhn, and A. Zrenner, *Phys. Rev. B* **73**, 125304 (2006)
 - [15] T. Flissikowski, A. Betke, I. A. Akimov, and F. Henneberger, *Phys. Rev. Lett.* **92**, 227401 (2004)
 - [16] P. Machnikowski, *Phys. Rev. B* **78**, 195320 (2008)
 - [17] J.-M. Gérard, B. Sermage, B. Gayral, B. Legrand, E. Costard, and V. Thierry-Mieg, *Phys. Rev. Lett.* **81**, 1110 (1998)
 - [18] F. P. Laussy, E. del Valle, and C. Tejedor, *Phys. Rev. B* **79**, 235325 (2009)
 - [19] J. Eberly and K. Wódkiewicz, *J. Opt. Soc. Am.* **67**, 1252 (1977)
 - [20] J. Wiersig, C. Gies, F. Jahnke, M. Aßmann, T. Berstermann, M. Bayer, C. Kistner, S. Reitzenstein, C. Schneider, S. Höfling, A. Forchel, C. Kruse, J. Kalden, and D. Homme, *Nature* **460**, 245 (2009)